REPORT DOCUMENTATION PAGE

Form Approved
OMB No. 0704-0188

1. REPORT DATE (DD-MM-YYYY)	2. REPORT TYPE	3. DATES COVERED (From - To)
2000	Open Literature	

4. TITLE AND SUBTITLE
Alterations in Inflammatory Cytokine Gene Expression in Sulfur Mustard-exposed Mouse Skin

5a. CONTRACT NUMBER

5b. GRANT NUMBER
DAAL30-C-91-10034

5c. PROGRAM ELEMENT NUMBER

6. AUTHOR(S)
Sabourin, C.L.K., Petrali, J.P., and Casillas, R.P.

5d. PROJECT NUMBER

5e. TASK NUMBER

5f. WORK UNIT NUMBER

7. PERFORMING ORGANIZATION NAME(S) AND ADDRESS(ES)

Division of Environ. Health Sciences, School of Public Health, Ohio State University, Columbus, OH
AND
USAMRICD
ATTN: MCMR-UV-CC
5100 Ricketts Point Road
Aberdeen Proving Ground, MD
21010-5400

8. PERFORMING ORGANIZATION REPORT NUMBER
USAMRICD-P00-011

9. SPONSORING / MONITORING AGENCY NAME(S) AND ADDRESS(ES)
US Army Medical Research Institute of Chemical Defense
ATTN: MCMR-UV-RC
3100 Ricketts Point Road
Aberdeen Proving Ground, MD
21010-5400

10. SPONSOR/MONITOR'S ACRONYM(S)

11. SPONSOR/MONITOR'S REPORT NUMBER(S)

12. DISTRIBUTION / AVAILABILITY STATEMENT
Approved for public release; distribution unlimited

13. SUPPLEMENTARY NOTES
Published in Journal of Biochemistry and Molecular Toxicology, 14(6), 291-301, 2000

14. ABSTRACT
See reprint.

15. SUBJECT TERMS
sulfur mustard (HD), bis(2-chloroethyl)sulfide, skin, inflammation, mouse, cytokine, gene expression, RT-PCR, immunohistochemistry, in vivo, animal model

16. SECURITY CLASSIFICATION OF:			17. LIMITATION OF ABSTRACT	18. NUMBER OF PAGES	19a. NAME OF RESPONSIBLE PERSON
a. REPORT	b. ABSTRACT	c. THIS PAGE			John P. Petrali
UNCLASSIFIED	UNCLASSIFIED	UNCLASSIFIED	UNLIMITED	11	19b. TELEPHONE NUMBER (include area code) 410-436-2334

J BIOCHEM MOLECULAR TOXICOLOGY
Volume 14, Number 6, 2000

Alterations in Inflammatory Cytokine Gene Expression in Sulfur Mustard–Exposed Mouse Skin

Carol L. K. Sabourin,[1] John P. Petrali,[2] and Robert P. Casillas[2]

[1]Division of Environmental Health Sciences, School of Public Health, The Ohio State University, Columbus, OH 43210
[2]United States Army Medical Research Institute of Chemical Defense, Aberdeen Proving Ground, MD 21010

Received 2 February 2000; revised 30 May 2000; accepted 5 June 2000

ABSTRACT: Cutaneous exposure to sulfur mustard (bis(2-chloroethyl) sulfide, HD), a chemical warfare agent, produces a delayed inflammatory skin response and severe tissue injury. Despite defined roles of inflammatory cytokines produced or released in response to skin-damaging chemicals, in vivo cytokine responses associated with HD-induced skin pathogenesis are not well understood. Additionally, there is little information on the in vivo temporal sequence of gene expression of cytokines postexposure to HD. The goal of these studies was to identify in vivo molecular biomarkers of HD skin injury within 24 hours after HD challenge. Gene expression of interleukin 1β (IL-1β), granulocyte-macrophage colony stimulating factor (GM-CSF), interleukin 6 (IL-6), and interleukin 1α (IL-1α) in the mouse ear vesicant model was examined by quantitative reverse transcription–polymerase chain reaction (RT-PCR). An increase in IL-1β mRNA levels was first observed at 3 hours. IL-1β, GM-CSF, and IL-6 mRNA levels were dramatically increased at 6–24 hours postexposure. IL-1α mRNA levels were not increased following HD exposure. Immunohistochemical studies demonstrated that IL-1β and IL-6 protein was produced at multiple sites within the ear, including epithelial cells, inflammatory cells, hair follicles, sebaceous glands, the dermal microvasculature, smooth muscle, and the dermal connective tissue. An increase in the intensity of staining for IL-1β and IL-6 was observed in localized areas at 6 hours and was evident in multiple areas at 24 hours. Positive staining for GM-CSF immunoreactive protein was localized to the inflammatory cells within the dermis. The number of immunostaining cells was increased as early as 1 hour following HD exposure. These studies document an early increase in the in vivo expression of inflammatory cytokines following cutaneous HD exposure. An understanding of the in vivo cytokine patterns following HD skin exposure may lead to defining the pathogenic mechanisms of HD injury and the development of pharmacological countermeasures. © 2000 John Wiley & Sons, Inc. J Biochem Mol Toxicol 14:291–302, 2000

KEY WORDS: **Sulfur Mustard (HD); Bis(2-chloroethyl)sulfide; Skin; Inflammation; Mouse; Cytokine; Gene Expression; RT-PCR; Immunohistochemistry; In Vivo; Animal Model**

INTRODUCTION

Sulfur mustard (bis(2-chloroethyl)sulfide, HD) produces incapacitating injury to the skin of exposed individuals. However, cutaneous exposure to HD does not cause immediately noticeable effects. Onset and severity of skin injury is dependent on dose, skin moisture, body site, and ambient temperature. Erythema appears within a few hours of exposure followed by edema and blister formation [1]. Histopathologically, cutaneous exposure to HD in animal or man is characterized by edema, dermal infiltration of inflammatory cells, premature death of basal layer epidermal cells, and epidermal–dermal separation [2–10]. Although cutaneous histopathological markers are useful endpoints of HD exposure, the role of inflammatory mediators produced prior to this endpoint is important for a better understanding of the mechanism(s) of action of HD.

In previous studies, we observed an inflammatory response in the mouse ear following topical exposure with liquid HD [11]. Histopathologically, the mouse ear vesicant model (MEVM) produced a mild inflammatory infiltrate similar to what is seen in human skin [9]. The MEVM provides quantification of the cutaneous inflammatory response following HD exposure by measuring ear swelling. Further studies using the

Correspondence to: Dr. Robert Casillas. Present address: Battelle Memorial Institute, 505 King Avenue, Columbus, OH 43201-2693; Tel: 614-424-5102; Fax: 614-424-3317; E-mail: casillasr@battelle.org

Contract Grant Sponsor: United States Army Medical Research Institute of Chemical Defense.
Contract Grant Number: DAAL30-C-91-0034.
A portion of this work was presented at the 37th Annual Meeting of the Society of Toxicology, March 1998.

MEVM identified the in vivo production of the cytokine interleukin 6 (IL-6) protein in cutaneous tissue from the ear [12]. The goal of the current study was to utilize the MEVM to identify in vivo biological markers for quick and accurate assessment of HD-induced skin injury, which may be used to corroborate noninvasive endpoints and histopathological alterations. The identification and characterization of the cellular products that regulate the activation and migration of inflammatory cells into the dermis and potentially result in the destruction of basal epidermal cells will provide insights into the selective targeting of medical countermeasures against these processes.

Cytokines are known to play a major role in acute and chronic inflammation. Furthermore, granulocyte-macrophage colony stimulating factor (GM-CSF), interleukin 1 (IL-1), and IL-6 are known to act through a network in various biological processes including cell growth and differentiation, immunoregulation, and inflammation. In vivo studies have demonstrated that GM-CSF and IL-1α induce the directed migration of neutrophils [13–15]. Few studies with in vivo HD skin models, including those conducted in our laboratory, have demonstrated the presence or addressed the role of inflammatory cytokines following direct cutaneous damage from HD [12,16]. Other investigators have shown that sulfur mustard does induce soluble cytokine responses in ex vivo skin models [17–19] and in vitro in human keratinocytes [20–23]. In this study we identified individual inflammatory cytokines and the temporal sequence of their expression in vivo in mouse ear skin exposed to HD. IL-1β, GM-CSF, IL-6, and IL-1α gene expression was examined by quantitative reverse-transcription polymerase chain reaction (RT-PCR), and protein expression was localized by immunohistochemistry. The expression of these mediators will be used for the continued development of quantifiable in vivo biological markers in response to HD injury and to evaluate the effectiveness of medical countermeasures.

MATERIALS AND METHODS

HD Cutaneous Exposure

Male CD1 mice, approximately four weeks of age, were purchased from Charles River Laboratories (Raleigh, NC) and housed in a controlled environment with a 12 hour light/dark cycle. Purina Certified Rodent Chow and water was available ad libitum. Animals were maintained under an Association for Assessment and Accreditation of Laboratory Animal Care (AAALAC) International program. On the study day, mice weighing in the range of 25–35 g were marked for identification and anesthetized with a combination of ketamine (60 mg/kg) and xylazine (12 mg/kg) by intraperitoneal injection. In a fume hood, a single application of 5 μL of 390 mM HD (0.32 mg) in dichloromethane was applied to the inner surface of the right ear according to published procedures [11]. This volume of HD allowed even distribution of agent over the entire medial surface of the ear. The left ear (vehicle control) was only exposed to 5 μL of dichloromethane. Animals were housed individually after HD challenge, and cages were placed on warm water-perfused heating pads within the laboratory fume hood system. At 1, 3, 6, 12, 18, and 24 hours post–HD challenge, animals were euthanized in a halothane-filled chamber. Both ears (1 HD-exposed and 1 vehicle control ear) were collected from two animals per time period. Each ear tissue was then bisected into two portions. One portion of each ear tissue was immediately fixed in 10% neutral buffered formalin, rinsed in PBS, processed, and then embedded in paraffin blocks. The other portion was immediately snap frozen in liquid nitrogen and stored at −80°C for RNA isolation.

RNA Isolation

Total cellular RNA was isolated from previously frozen tissues by using TRIzol Reagent (Life Technologies, Gaithersburg, MD). Tissue was homogenized with TRIzol using a polytron homogenizer. PhaseLock Gel (5 Prime 3 Prime, Inc., Boulder, CO) was used during centrifugation to allow separation of the phenol–chloroform phase from the aqueous phase. The aqueous phase was transferred to a fresh tube, and isopropanol was added to precipitate the RNA. The sample was centrifuged, and the pellet washed with 75% ethanol. The RNA pellet was dissolved in 100 μL of diethyl pyrocarbonate (DEPC) treated water. To reduce the percentage of contaminating DNA, a second RNA extraction using TRIzol reagent was performed. 900 μL of TRIzol reagent was added to the 100 μL of RNA sample, and the extraction was repeated. The final RNA pellet was resuspended in 50 μL of DEPC-treated water. RNA was quantitated spectrophotometrically based an absorbance at 260 nm of 1 equal to an RNA concentration of 40 μg/mL. The RNA samples were analyzed for integrity of 18S and 28S ribosomal RNA (rRNA) by ethidium bromide staining of 1.0 μg of RNA resolved by electrophoresis on a 1.0% agarose gel in Tris-borate-EDTA (45 mM Tris-borate, pH 8.0, 1 mM EDTA).

RT-PCR

RNA was incubated at 60°C for 10 minutes and chilled to 4°C immediately before being reverse-tran-

TABLE 1. Primer Sequences

Primer[a,b]	*Sequence*	*Nucleotides*[c]	*Fragment*	*Cycles*
IL-1β S	5′ATGGCAACTGTTCCTGAACTCAACT3′	78–102	563 bp	30
IL-1β AS	5′CAGGACAGGTATAGATTCTTTCCTTT3′	615–640		
GM-CSF S	5″TGTGGTCTACAGCCTCTCAGCAC3′	64–86	368 bp	35
GM-CSF AS	5′CAAAGGGGATATCAGTCAGAAAGGT3′	407–431		
IL-6 S	5′ATGAAGTTCCTCTCTGCAAGAGACT3′	34–57	638 bp	38
IL-6 AS	5′CACTAGGTTTGCCGAGTAGATCTC3′	648–671		
IL-1α S	5′AAGATGTCCAACTTCACCTTCAAGGAGAGCCG3′	241–272	491 bp	30
IL-1α AS	5′AGGTCGGTCTCACTACCTGTGATGAGTTTTGG3′	700–731		
HPRT S	5′GTAATGATCAGTCAACGGGGGAC3′	404–426	177 bp	29
HPRT AS	5′CCAGCAAGCTTGCAACCTTAACCA3′	557–580		

[a]IL, interleukin; GM-CSF, granulocyte-macrophage colony stimulating factor; HPRT, hypoxanthine-guanine phosphoribosyltransferase.
[b]S, sense; AS, antisense.
[c]Nucleotide position according to GenBank sequence.

scribed. Reverse transcription of 4 μg of total RNA was performed in a volume of 40 μL containing 100 units of SuperScript II RNase H⁻ Reverse Transcriptase (Life Technologies), 10 mM Tris HCl, pH 8.3, 50 mM KCl, 5 mM $MgCl_2$, 1 unit/μL RNasin (Promega Corp., Madison, WI), 1 mM each of dATP, dGTP, dCTP, and dTTP, and 200 pmol of random hexamers (Life Technologies) for 60 minutes at 37°C. The samples were incubated for 10 minutes at 25°C before transcription and heated to 99°C for 5 minutes to terminate the reverse transcription reaction.

By using a Perkin-Elmer DNA Thermocycler 9600 (Perkin-Elmer, Norwalk, CT), 2 μL of cDNA mixture obtained from the reverse transcription reaction was amplified for the specific genes. The amplification reaction mixture consisted of 10 mM Tris HCl, pH 8.3; 50 mM KCl; 2.5 mM $MgCl_2$; 0.2 mM each of dATP, dGTP, dCTP, and dTTP; 0.25 μM each of sense and antisense primers; and 0.625 units of Taq DNA polymerase (Life Technologies) in a final volume of 25 μL. The Taq DNA polymerase was preincubated with TaqStart antibody (Clontech, Palo Alto, CA) for 5 minutes at room temperature. Water and reverse transcriptase minus reactions were run as negative controls. The reaction mixture was first heated at 95°C for 30 seconds, and amplification was at 95°C for 15 seconds, 60°C for 30 seconds, and 72°C for 30 seconds, followed by incubation for 7 minutes at 72°C. The PCR primers and fragment sizes are listed in Table 1. The PCR products were electrophoresed through a 1.8% agarose gel in Tris-borate-EDTA buffer and stained with ethidium bromide.

Quantitative PCR Analysis

PCR MIMICs for mouse IL-1β, GM-CSF, IL-6, and IL-1α were purchased from Clontech (Palo Alto, CA). A PCR MIMIC for mouse hypoxanthine–guanine phosphoribosyltransferase (HPRT) was constructed using the PCR MIMIC Construction Kit (Clontech) according to the manufacturer's instructions with the composite primers HPRT Sense 5′-CTAATGATCAGTCAACGGGGGACGCAGATGAGTATCTTGTCCC-3′ and HPRT Antisense 5′-CCAGCAAGCTTGCAACCTTAACCAATTTGATTCTGGACCATGGC-3′. Competitive PCR was carried out to quantitate the relative changes in mRNA. The appropriate range of PCR MIMIC was determined using 10-fold dilutions of the PCR MIMIC. PCR was then performed with reverse transcribed RNA, containing five to seven 2-fold dilutions of PCR MIMIC. Aliquots were electrophoresed on a 1.8% agarose gel in Tris-borate-EDTA and stained with ethidium bromide. A CCD image sensor (Alpha Innotech Corporation, San Leandro, CA) measured the intensity of ethidium bromide luminescence. A log–log plot of the ratio of cytokine target peak area to cytokine MIMIC peak area versus the molar amount of cytokine MIMIC added to the PCR reaction was constructed. Linear regression analysis was performed. The molar amount of cytokine target cDNA from the reverse transcribed RNA was determined from the intersection of the curve with a ratio of 1.0 to the x-axis. The mRNA level of cytokine was expressed in attomol/μg RNA. A similar analysis was performed for HPRT. The attomol/μg of each cytokine was normalized to the attomol/μg of HPRT.

Immunohistochemical Staining

Skin specimens collected from two animals (one HD-exposed and one vehicle-control-exposed site per animal) per time period for six time periods (1, 3, 6, 12, 18, and 24 hours) were used for immunohistochemical evaluation. Paraffin-embedded tissue sections (5 μM each) were deparaffinized and rehydrated. Endogenous peroxidase activity was ablated with 1% hydrogen peroxide in PBS. Tissue sections were washed in PBS. GM-CSF immunostained tissue sections were in-

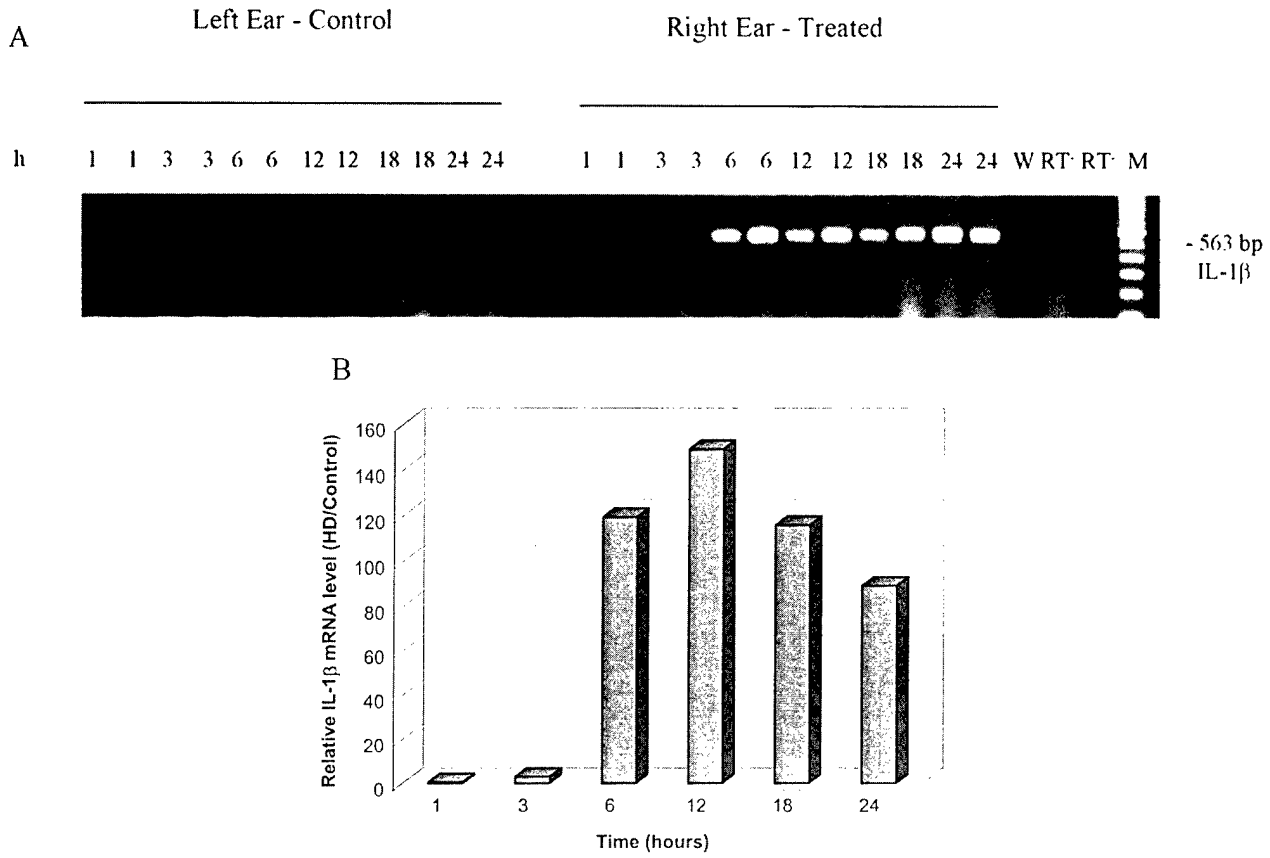

FIGURE 1. IL-1β gene expression in control and HD-exposed mouse ear from 1 to 24 hours postexposure. RNA was isolated from vehicle-control-treated (dichloromethane) and HD-treated mouse ear. RNA was reverse transcribed followed by amplification of cytokine cDNA. (A) The PCR product was loaded onto a 1.8% agarose gel, resolved by electrophoresis, and visualized by staining with ethidium bromide. RT , no reverse transcriptase; W, water control; and M, 100 base pair marker. (B) Analysis of relative changes in IL-1β mRNA levels determined by competitive PCR. Aliquots of cDNA were amplified in presence of 2-fold dilutions of IL-1β MIMICs. After PCR was performed, aliquots were electrophoresed on a 1.8% agarose gel. The peak areas of the bands corresponding to the IL-1β mRNA in mouse skin and IL-1β MIMICs were determined by image analysis. Attomol/μg RNA for IL-1β was determined as detailed in the Materials and Methods. Attomol/μg for IL-1β was normalized to the attomol/μg for the housekeeping gene HPRT for each sample. HD-treated skin normalized IL-1β levels were divided by the dichloromethane-treated skin normalized IL-1β levels. The average of two separate determinations was plotted for the 24 hour time course.

cubated with 0.1% trypsin (bovine pancreas type III, Sigma, St. Louis, MO) for 30 minutes at 37°C and subsequently washed three times with PBS. PBS containing 10% normal rabbit serum (GM-CSF and IL-6) or 10% normal goat serum (IL-1β) was used to suppress nonspecific protein binding. Tissue sections were incubated overnight at 4°C with the primary antibodies monoclonal rat anti-mouse GM-CSF, polyclonal rabbit anti-mouse IL-1β, or monoclonal rat anti-mouse IL-6 (Genzyme, Cambridge, MA). The sections were washed with PBS and incubated with biotinylated rabbit anti-rat IgG (GM-CSF and IL-6) or goat anti-rabbit IgG (IL-1β), (Vector Laboratories, Burlingame, CA) at a dilution of 1:100 for 30 minutes at room temperature. After washing, the sections were incubated with avidin–biotin peroxidase complex at room temperature for 30 minutes using the Vectastain Elite ABC kit (Vector Laboratories). Color was developed with 3,3'-diaminobenzidine tetrahydrochloride (DAB) as the substrate. The sections were counterstained with Harris' acid hematoxylin (Shandon, Pittsburgh, PA). To demonstrate specificity of the immunostaining, the primary antibodies were replaced with similar protein concentrations of antibody neutralized with the recombinant cytokines (Genzyme) at 37°C, and no primary antibody. Slides were evaluated by light microscopy, and representative areas were photographed.

RESULTS

Quantitative RT-PCR Analysis: Effect of HD on Cytokine Gene Expression

Studies were performed to determine the time dependence of induction of inflammatory cytokine gene

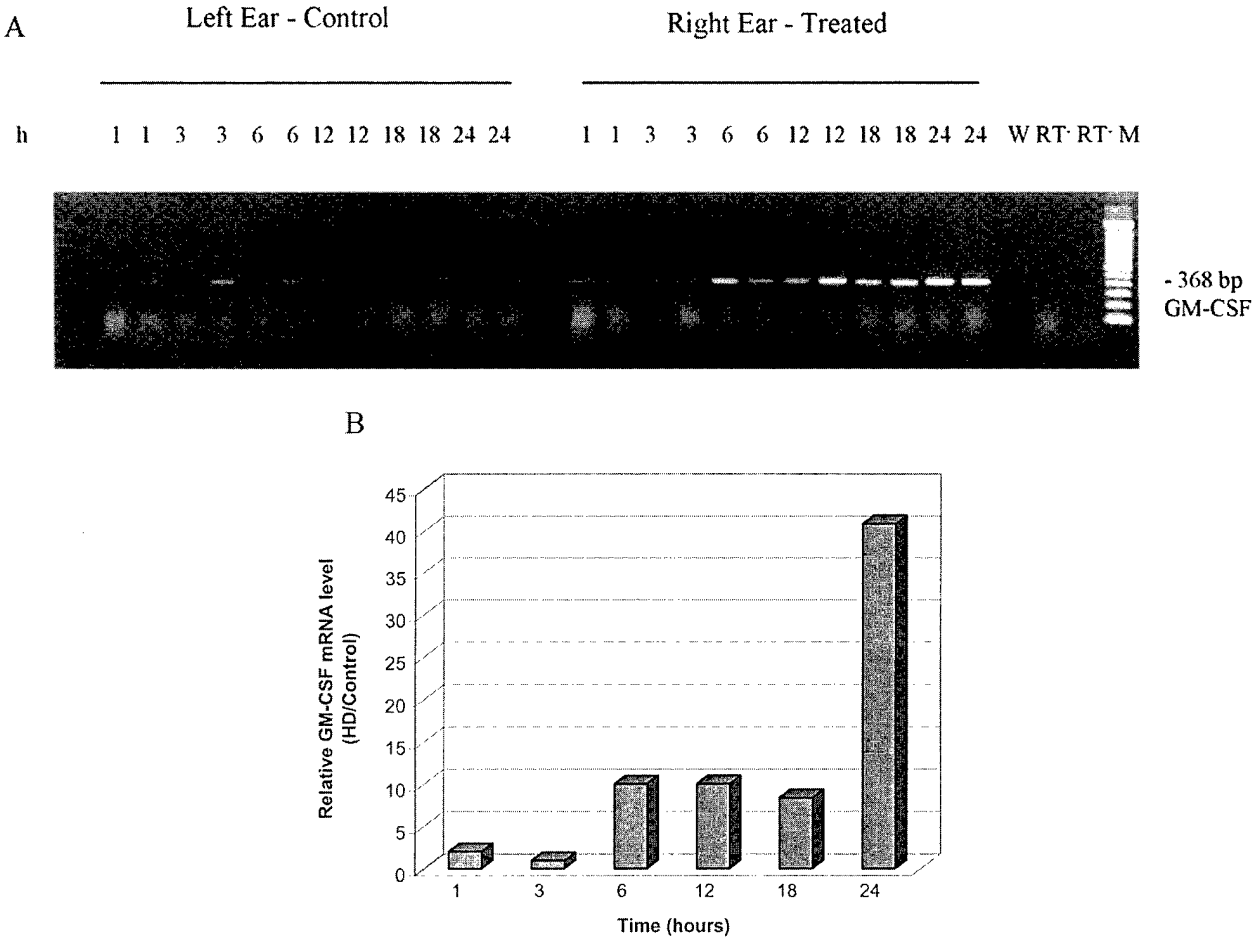

FIGURE 2. GM-CSF gene expression in control and HD-exposed mouse ear from 1 to 24 hours postexposure. RNA was isolated from vehicle-control-treated (dichloromethane) and HD-treated mouse ear. RNA was reverse transcribed followed by amplification of cytokine cDNA. (A) The PCR product was loaded onto a 1.8% agarose gel, resolved by electrophoresis, and visualized by staining with ethidium bromide. RT^-, no reverse transcriptase; W, water control; and M, 100 base pair marker. (B) Analysis of relative changes in GM-CSF mRNA levels determined by competitive PCR. Aliquots of cDNA were amplified in presence of 2-fold dilutions of GM-CSF MIMICs. After PCR was performed, aliquots were electrophoresed on a 1.8% agarose gel. The peak areas of the bands corresponding to the GM-CSF mRNA in mouse skin and GM-CSF MIMICs were determined by image analysis. Attomol/μg RNA for GM-CSF was determined as detailed in Materials and Methods. Attomol/μg for GM-CSF was normalized to the attomol/μg for the housekeeping gene HPRT for each sample. HD-treated skin normalized GM-CSF levels were divided by the dichloromethane-treated skin normalized GM-CSF levels. The average of two separate determinations was plotted for the 24 hour time course.

expression over a time period of 1–24 hours in CD1 mouse ears following topical HD exposure. IL-1β, GM-CSF, IL-6, and IL-1α gene expression was examined by RT-PCR to establish the in vivo cytokine pattern (Figures 1–4A). Amplification of HPRT was similar in tissue from control and HD-exposed mouse ear at all time periods (Figure 5A). Quantitation of the relative changes in gene expression for cytokines and HPRT was accomplished by competitive PCR using PCR MIMICs as illustrated for HPRT (Figure 5B and C).

Gene expression in control mouse ear was detectable for all inflammatory cytokines except IL-6. In HD-exposed ears, a time-dependent increase in IL-1β, GM-CSF, and IL-6 mRNA levels (Figures 1–3) was observed following a single application of 5 μL of 390 mM HD in dichloromethane on the inner surface of the ear. IL-1β mRNA levels were moderately increased from control levels at 3 hours postexposure to HD (Figure 1), however, there was an increase of greater than 100-fold at 6 hours compared to control levels. GM-CSF mRNA levels were increased 10-fold from control levels at 6 hours postexposure to HD and were increased 40-fold at 24 hours (Figure 2). An IL-6 PCR product was first observed at 6 hours postexposure to HD with no further increase in the IL-6 mRNA levels from 6 to 24 hours (Figure 3). IL-1α mRNA levels were relatively unaltered over the time period of 1–24 hours following topical treatment with HD (Figure 4).

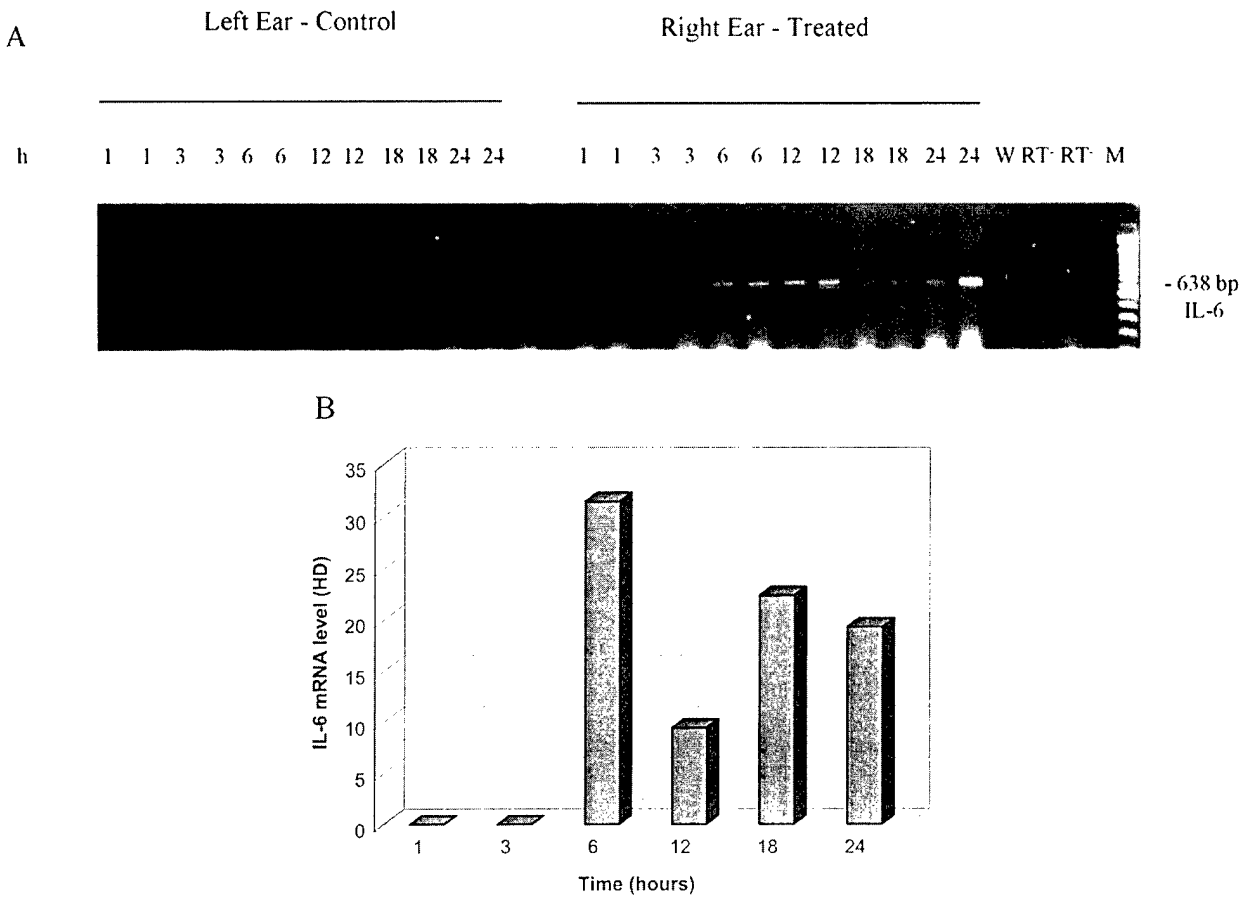

FIGURE 3. IL-6 gene expression in control and HD-exposed mouse ear from 1 to 24 hours postexposure. RNA was isolated from vehicle-control-treated (dichloromethane) and HD-treated mouse ear. RNA was reverse transcribed followed by amplification of cytokine cDNA. (A) The PCR product was loaded onto a 1.8% agarose gel, resolved by electrophoresis, and visualized by staining with ethidium bromide. A PCR product for IL-6 was not detected in dichloromethane-treated skin. RT , no reverse transcriptase; W, water control; and M, 100 base pair marker. (B) Analysis of IL-6 mRNA levels determined by competitive PCR. Aliquots of cDNA were amplified in presence of 2-fold dilutions of IL-6 MIMICs. After PCR was performed, aliquots were electrophoresed on a 1.8% agarose gel. The peak areas of the bands corresponding to the IL-6 mRNA in mouse skin and IL-6 MIMICs were determined by image analysis. Attomol/μg RNA for IL-6 was determined as detailed in Materials and Methods. Attomol/μg for IL-6 was normalized to the attomol/μg for the housekeeping gene HPRT for each sample. The average of two separate determinations was plotted for the 24 hour time course.

Immunohistochemical Localization of Cytokine Expression

Immunohistochemical studies were performed to identify the cell types within the epidermis and dermis that produced the cytokines in response to topical application of HD over the 24 hour time course. Immunostaining of IL-1β was localized to multiple sites within the ear including epithelial cells, inflammatory cells, adnexal structures (hair follicles and sebaceous glands), the dermal microvasculature, smooth muscle, and the dermal connective tissue. Staining was similar in control and HD-exposed mouse ears at 1 and 3 hours. Beginning at 6 hours postexposure, localized areas with increased IL-1β immunostaining were observed in the HD-treated ears. The cutaneous tissue showed intense staining for IL-1β immunoreactive protein in multiple areas at 24 hours posttreatment with HD (Figure 6A and B).

Immunostaining of GM-CSF over the 24 hour time course was localized to the dermal inflammatory cells. In general, few cells stained positive in the control ears. An increase in the number of inflammatory cells staining positive for GM-CSF was observed beginning at 1 hour post–HD challenge and continued throughout the time course. Figure 6C and D illustrates the pattern of cells staining for GM-CSF immunoreactive protein compared to control at the 6 hour time point.

Immunostaining of IL-6 was localized to multiple sites within the ear, including epithelial cells, inflammatory cells, adnexal structures (hair follicles and sebaceous glands), the dermal microvasculature, smooth muscle, and the dermal connective tissue. Staining was

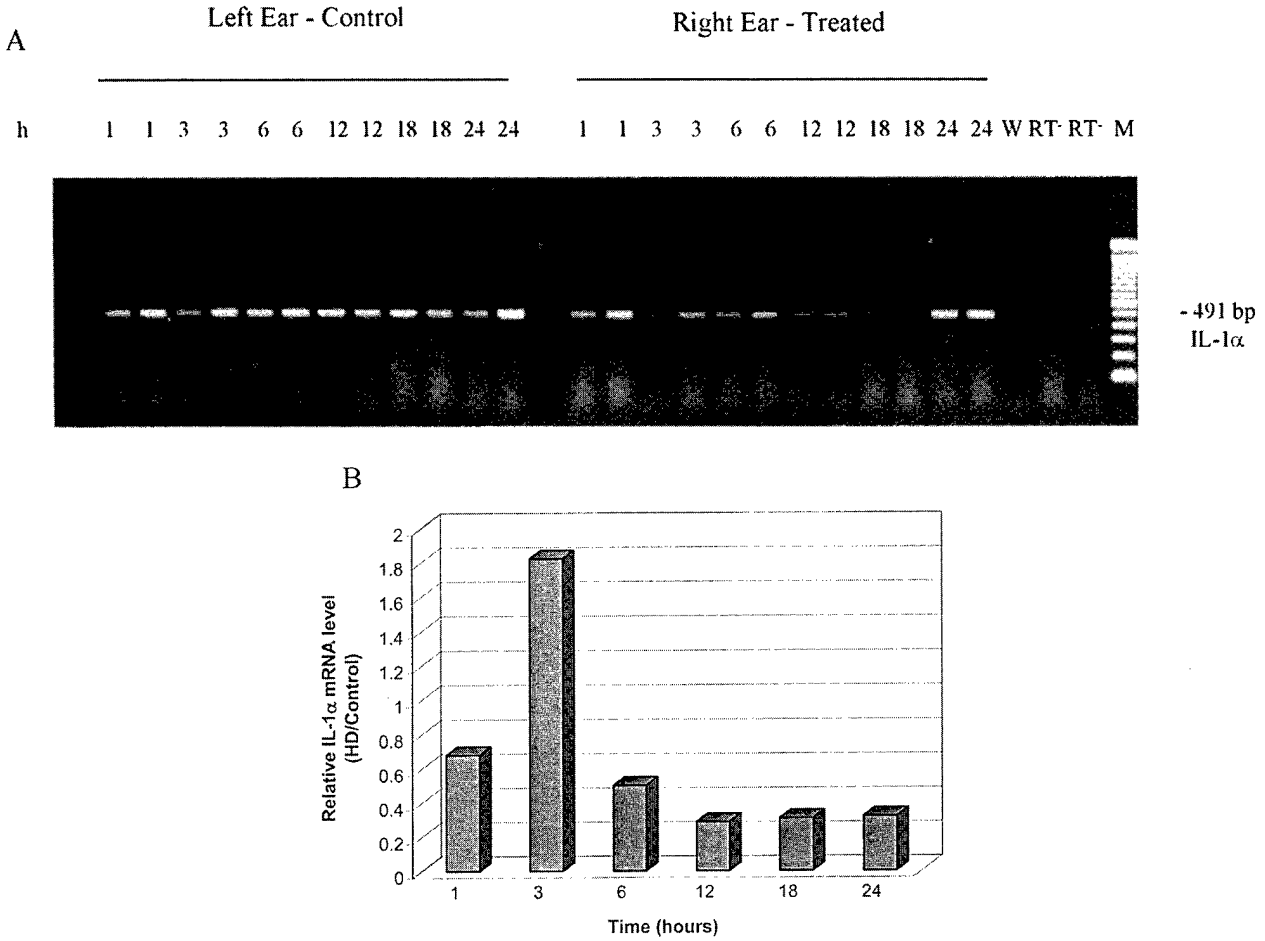

FIGURE 4. IL-1α gene expression in control and HD-exposed mouse ear from 1 to 24 hour postexposure. RNA was isolated from vehicle-control-treated (dichloromethane) and HD-treated mouse ear. RNA was reverse transcribed followed by amplification of cytokine cDNA. (A) The PCR product was loaded onto a 1.8% agarose gel, resolved by electrophoresis, and visualized by staining with ethidium bromide. RT^-, no reverse transcriptase; W, water control; and M, 100 base pair marker. (B) Analysis of relative changes in IL-1α mRNA levels determined by competitive PCR. Aliquots of cDNA were amplified in presence of 2-fold dilutions of IL-1α MIMICs. After PCR was performed, aliquots were electrophoresed on a 1.8% agarose gel. The peak areas of the bands corresponding to the IL-1α mRNA in mouse skin and IL-1α MIMICs were determined by image analysis. Attomol/μg RNA for IL-1α was determined as detailed in Materials and Methods. Attomol/μg for IL-1α was normalized to the attomol/μg for the housekeeping gene HPRT for each sample. HD-treated skin normalized IL-1α levels were divided by the dichloromethane-treated skin normalized IL-1α levels. The average of two separate determinations was plotted for the 24 hour time course.

similar in control and HD-exposed mouse ears at early time points, however, at 6 hours, staining intensity was increased in the HD-exposed ear. The epithelium of the HD-treated ear showed intense staining for IL-6 immunoreactive protein at 24 hours (Figure 6E and F).

DISCUSSION

This study defined the temporal sequence of gene expression of the inflammatory cytokines IL-1β, GM-CSF, IL-6, and IL-1α following a single topical exposure to HD. These data document for the first time the use of quantitative RT-PCR and immunohistochemistry to establish an in vivo cytokine pattern in mouse skin exposed to HD. Furthermore, these data demonstrate that damage to the skin by HD results in an immunological response characterized by specific and increased cytokine gene expression. These cytokines are known to function in maintaining cutaneous homeostasis and play a key role in the pathogenesis of a number of dermatological diseases [24–27]. GM-CSF and IL-1 act as potent chemoattractant factors, either directly or by stimulating the production of chemokines that recruit inflammatory leukocytes to sites of inflammation [14,28,29]. IL-1 can induce the expression of adhesion molecules, including intercellular adhesion molecule-1 (ICAM-1) on the surface of vascular endothelial cells [14,28]. Cutaneous production of these cytokines in response to HD-induced injury suggests

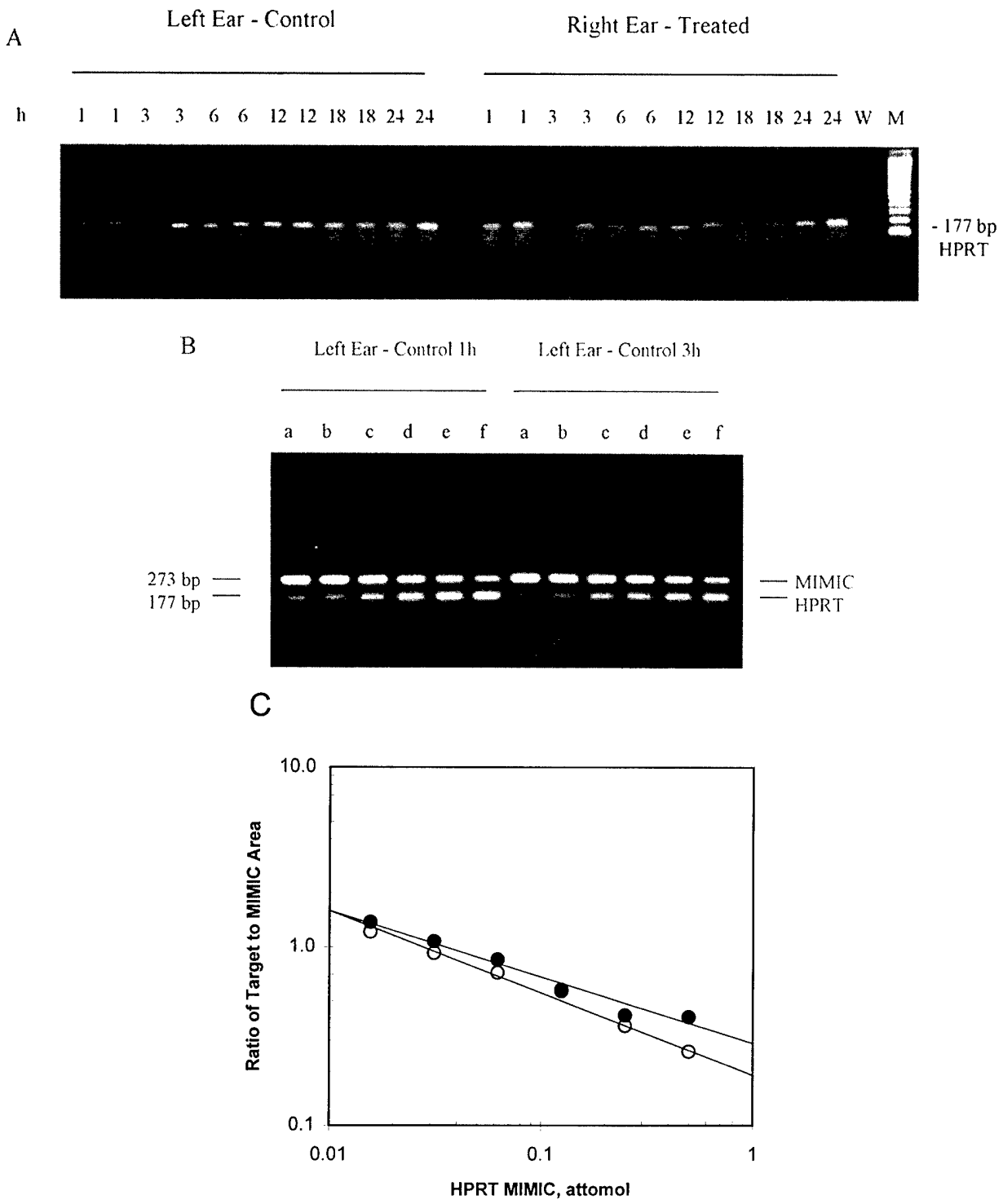

FIGURE 5. (A) HPRT gene expression in control and HD-exposed mouse ear from 1 to 24 hour postexposure. RNA was isolated from vehicle-control-treated (dichloromethane) and HD-treated mouse ear. RNA was reverse transcribed followed by amplification of cytokine cDNA. The PCR product was loaded onto a 1.8% agarose gel, resolved by electrophoresis, and visualized by staining with ethidium bromide. RT , no reverse transcriptase; W, water control; and M, 100 base pair marker. (B) Competitive PCR analysis of changes in HPRT mRNA levels in mouse ear control samples at 1 and 3 hours. PCR was carried out using 0.1 μg of reverse-transcribed total RNA in the presence of 2-fold dilutions of HPRT MIMIC. The PCR products were resolved on a 1.8% agarose gel and stained with ethidium bromide. The HPRT target was 177 bp (lower band), and the HPRT MIMIC was 273 bp (upper band). The following amounts of HPRT MIMIC were used in the reaction: 5.0×10^{1} attomol, lane a; 2.5×10^{-1} attomol, lane b; 1.25×10^{-1} attomol, lane c; 6.25×10^{2} attomol, lane d; 3.12×10^{2} attomol, lane e; and 1.56×10^{2} attomol, lane f. M, 100 bp marker. (C) Graphic analysis of the quantitative PCR analysis shown in B. The peak area of the electrophoretic bands was measured by image analysis. The closed and open circles denote data derived from 1 h and 3 hour control ear samples, respectively. The ratio of the target to MIMIC area was plotted against the attomol of HPRT MIMIC added to the PCR reaction. Lines were drawn based on a linear regression analysis of six data points. Left ear control for 1 hour was 0.035 attomol/0.1 μg RNA and left ear control for 3 hours was 0.027 attomol/0.1 μg RNA.

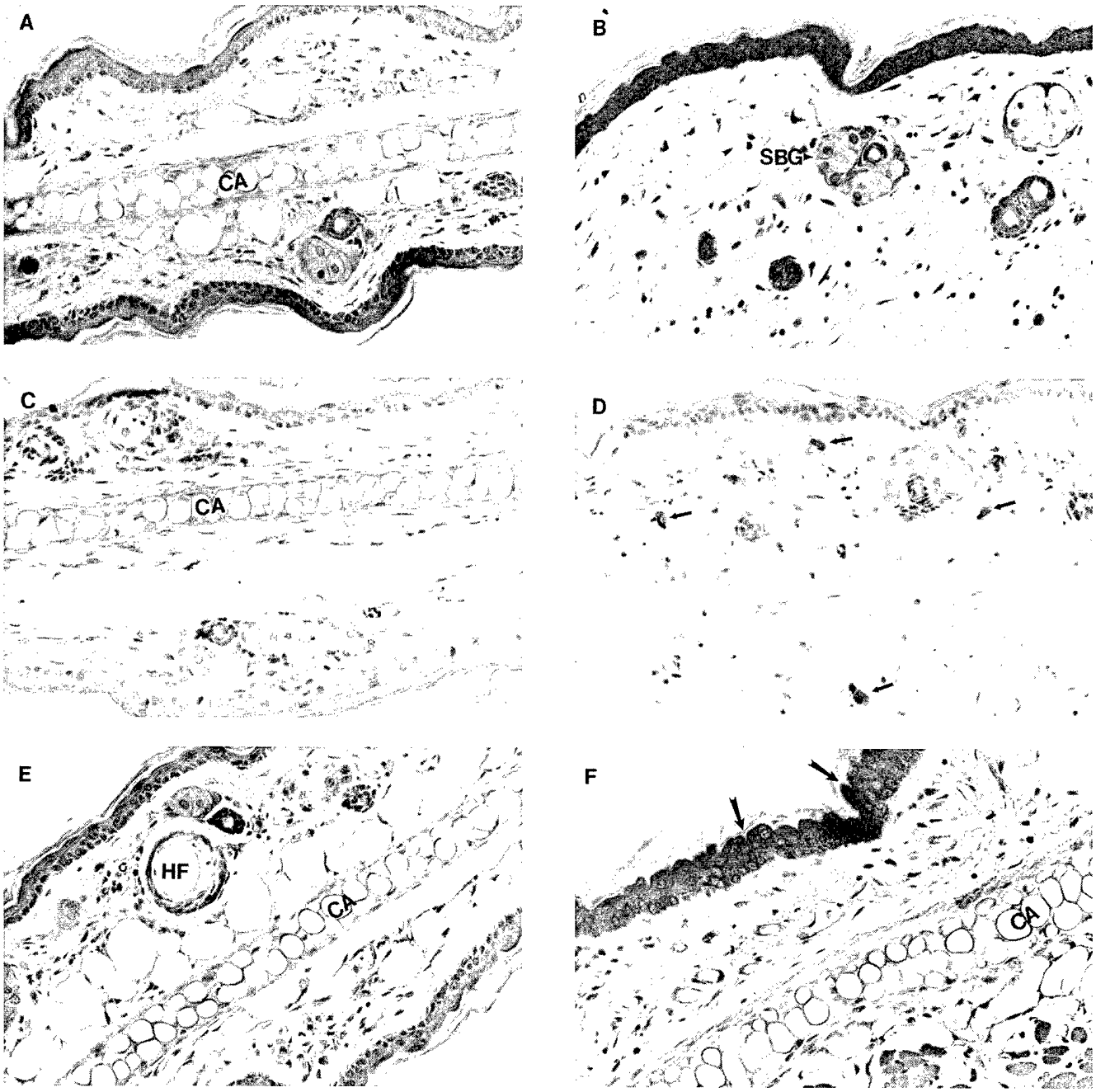

FIGURE 6. Immunohistochemical localization of protein for IL-1β in dichloromethane-treated (A) and HD-treated (B) mouse ear at 24 hours posttreatment; GM-CSF in dichloromethane-treated (C) and HD-treated mouse ear (D) at 6 hours posttreatment; and IL-6 in dichloromethane-treated (E) and HD-treated (F) mouse ear at 24 hours posttreatment. (A and B) IL-1β immunoreactive protein was localized to multiple sites, including epithelial cells, inflammatory cells, hair follicles, sebaceous glands, the dermal microvasculature, smooth muscle, and the dermal connective tissue. Immunostaining was light to moderate in control ear. HD-treatment resulted in increased IL-1β immunoreactive protein at 24 hours. Arrows indicate positive staining lymphocytes. CA, cartilage; SBG, sebaceous gland. Magnification 20X. (C and D) GM-CSF immunoreactive protein was localized to the inflammatory cells. An increase in the number of inflammatory cells containing immunoreactive GM-CSF protein in the HD-treated ear compared to the dichloromethane-treated ear was first observed at 1 hour posttreatment. Arrows indicate examples of positive-staining neutrophils. CA, cartilage. Magnification 20X. (E and F) IL-6 immunoreactive protein was localized to multiple sites including epithelial cells, inflammatory cells, hair follicles, sebaceous glands, the dermal microvasculature, smooth muscle, and the dermal connective tissue. Immunostaining was light to moderate in dichloromethane-treated mouse ear. HD treatment resulted in increased IL-6 immunoreactive protein at 24 hours. Large arrows indicate areas of epithelial degeneration, cytoplasmic staining of epithelial cells, elobulation of superior epithelial cells, and fibroblast staining. CA, cartilage; HF, hair follicle. Magnification 20X.

they may have a role in the increase of inflammatory cells at the site of HD exposure. Indeed, increased dermal inflammatory cells at the site of HD exposure is well established histopathologically in various animal skin models [3,9,30–35].

Quantitation of the relative changes in the mRNA levels was accomplished by competitive PCR using PCR MIMICs. In HD-exposed skin, mRNA expression for IL-1β was noticeably increased at 3 hours postexposure, whereas for GM-CSF and IL-6, noticeable increases began at 6 hours postexposure. IL-6 mRNA levels decreased from peak levels at 6 hours postexposure; however, mRNA levels remained at greater than 8-fold over basal levels during the 24 hour time course examined.

Immunohistochemical techniques were employed in order to correlate the alterations in cytokine mRNA levels with levels of protein subsequently produced. This also allowed for the localization of the cytokine proteins by the different cell types within the mouse skin. Immunostaining of GM-CSF was localized to the inflammatory cells independent of postexposure time. In general, few cells stained positive in the control ears, although there were localized regions of positive cells. IL-1β and IL-6 immunostaining was observed at multiple sites within the skin, including epidermal appendages and adnexal structures (hair follicles and sebaceous glands), the dermal microvasculature, smooth muscle, and the dermal connective tissue. Previous studies have localized IL-1β and IL-6 to these sites within human skin by in situ hybridization and immunohistochemistry [36–40]. An increase in the intensity of staining for IL-1β and IL-6 was first observed at 6 hours in the HD-exposed ear primarily in the epidermis.

The increase in mRNA expression for specific inflammatory mediators of HD skin damage, as early as 3 hours, clearly demonstrates that HD produces an early inflammatory response. These data are consistent with other studies in our laboratory that demonstrated, by ELISA, the early presence of the cytokine IL-6 by ELISA following in vivo HD injury in the mouse ear vesicant model and hairless mouse vesicant model [12]. The lack of increased IL-1α expression observed in the current study was consistent with recent findings in our laboratory where we demonstrated, by ELISA, no increase in IL-1α protein over a similar time course using the same mouse ear vesicant model challenged against liquid HD [12]. However in the hairless mouse vesicant model, we did observe by ELISA a time-dependent increase in IL-1α protein following topical exposure to HD vapor [12]. Further studies are needed to clarify what the pattern of IL-1α response is between these models and if the differences are due to strain, type of HD exposure, or site of exposure. The cutaneous inflammatory response has been considered a secondary event to HD injury and believed to play a role later in the injury phase (i.e., concurrent with or following histopathological damage) [1]. Our study clearly demonstrates that the time course of HD-induced inflammation precedes HD-induced histopathological damage (necrosis, subepidermal blister), which is known to occur after 12 hours postexposure in the mouse ear vesicant model using the same HD dose and dosing technique [11].

Currently, there is no therapeutic antidote against HD skin injury [1]. However, with the understanding that cutaneous inflammation could contribute to or exacerbate the pathogenesis of HD dermatotoxicity, it is reasonable to suggest that drugs preventing HD-induced inflammation would be prime candidates for therapeutic intervention. Indeed, our recent studies in the in vivo mouse ear vesicant model have demonstrated that topically applied anti-inflammatory drugs protect against acute HD-induced cutaneous inflammation and HD-induced subepidermal blisters [41]. Furthermore, we have shown systemically delivered anti-inflammatory drugs protect against HD-induced inflammation and pathological injury in vivo in the hairless mouse vesicant model [42].

In vivo studies with animal vesicant models have demonstrated the effectiveness of systemically delivered anti-inflammatory drugs against HD injury based on evaluation of survivability [43–44]. Protection from HD-induced inflammation has been observed following a systemic and topical combination treatment with corticosteroids in an in vivo rabbit vesicant model [45]. Conversely, an in vivo study with shaved guinea pigs showed no protection against HD-induced dermal lesions with systemically delivered prednisolone [46]. In an in vivo hairless guinea pig model, systemically administered niacinamide (NAM) and a systemic combination pretreatment with niacinamide, promethazine, and indomethacin protected against HD injury [47–49]. Interestingly, although NAM has traditionally been used in antivesicant research due to one of its pharmacological properties as a reversible inhibitor of poly(ADP-ribose)polymerase, NAM has known anti-inflammatory effects and is the active component of a topical medication, Papulex (GenDerm Canada Inc.), which is indicated as an antibiotic for the topical treatment of uncomplicated facial acne vulgaris. No protection against HD-induced pathology was observed ex vivo in human skin explants following treatment with niacinamide [50]. Similarly, in an ex vivo isolated pig flap model, no protection against subepidermal blisters was observed following perfusion with niacinamide; however, indomethacin did protect against HD-induced inflammatory mediators and pathological injury [51].

The results presented here demonstrate that in vivo damage to the skin by HD results in an immunological response defined by increased gene expression of the inflammatory cytokines IL-1β, GM-CSF, and IL-6 following a single topical exposure to HD. These findings are extremely useful for efforts to assess biochemical mediator targets in HD injury for intervention by pharmacological agents. In summary, intervention targeting the inflammatory response may not completely eliminate injury, but it may reduce the extent of the injury and thus decrease healing time.

ACKNOWLEDGMENTS

The authors thank Karen M. Ricketts, Theresa D. Doyel, and Donna L. Moltrup from the U.S. Army Medical Research Institute of Chemical Defense for their technical assistance. The opinions or assertions herein are the private views of the authors and are not to be construed as reflecting the views of the Department of the Army or the Department of Defense.

REFERENCES

1. Sidell, FR, Urbanetti JS, Smith WJ, Hurst CG. Vesicants. Textbook of military medicine; warfare, weaponry, and the casualty: medical aspects of chemical and biological warfare. In: Sidell FR, Takafuji ET, Franz DR, editors. Washington DC: TMM Publications; 1997. p 197–228.
2. Papirmeister B, Gross CL, Petrali JP, Hixson CJ. Pathology produced by sulfur mustard in human skin grafts on athymic nude mice: part I. Gross and light microscopic changes. J Toxicol Cutan Ocul Toxicol 1984;3:371–408.
3. Mitcheltree LW, Mershon MM, Wall HG, Pulliam JD. Microblister formation in vesicant-exposed pig skin. J Toxicol Cutan Ocul Toxicol 1989;8:309–319.
4. Petrali JP, Oglesby SB, Mills KR. Ultrastructural correlates of sulfur mustard toxicity. J Toxicol Cutan Ocul Toxicol 1990;9:193–214.
5. Mershon MM, Mitcheltree LW, Petrali JP, Braue EH, Wade JV. Hairless guinea pigs bioassay model for vesicant vapor exposures. Fund Appl Toxicol 1990;15:622–630.
6. Barranco VP. Mustard gas and the dermatologist. Int J Dermatol 1991;30:684–686.
7. Smith WJ, Dunn MA. Medical defense against blistering chemical warfare agents. Arch Dermatol 1991;127:1207–1213.
8. Borak J, Sidell FR. Agents of chemical warfare: sulphur mustard. Anal Emerg Med 1992;21:303–308.
9. Smith KJ, Casillas R, Graham J, Skelton HG, Stemler F, Hackley BE Jr. Histopathologic features seen with different animal models following cutaneous sulfur mustard exposure. J Dermatol Sci 1997;14:126–135.
10. Smith KJ, Smith WJ, Hamilton T, Skelton HG, Graham JS, Okerberg C, Moeller R, Hackley BE Jr. Histopathologic and immunohistochemical features in human skin after exposure to nitrogen and sulfur mustard. Am J Dermatopathol 1998;20:22–28.
11. Casillas RP, Mitcheltree LW, Stemler FW. The mouse ear model of cutaneous sulfur mustard injury. Toxicol Methods 1997;7:381–397.
12. Ricketts KM, Santai CT, France JA, Graziosi AM, Doyel TD, Gazaway MY, Casillas RP. Inflammatory cytokine response in sulfur mustard-exposed mouse skin. J Appl Toxicol, in press.
13. Wang JM, Chen ZG, Colella S, Bonilla MA, Welte K, Bordignon C, Mantovani A. Chemotactic activity of recombinant granulocyte colony stimulating factor. Blood 1988;72:1456–1460.
14. Sayers TJ, Wiltrout T, Bull CA, Denn AC, Pilaro AM, Lokesh B. Effects of cytokines on polymorphonuclear neutrophil infiltration in the mouse: prostaglandin- and leukotriene-independent induction of infiltration by IL-1 and tumor necrosis factor. J Immunol 1988;141:1670–1677.
15. Mason MJ, Van Epps DE. In vivo neutrophil emigration in response to interleukin-1 and tumor necrosis factor. J Leukemia Biol 1989;45:62–68.
16. Tsuruta J, Sugisaki K, Dannenberg AM Jr, Yoshimura T, Abe Y, Mounts P. The cytokines NAP-1 (IL-8), MCP-1, IL-1 beta, and GRO in rabbit inflammatory skin lesions produced by the chemical irritant sulphur mustard. Inflammation 1996;20:293–318.
17. Rikamaru T, Nakamura M, Yano T, Beck G, Habicht GS, Rennie LL, Widra M, Hirshman CA, Boulay MG, Spannhake EW, Lazarus GS, Pula PJ, Dannenberg AM. Mediators initiating the inflammatory response released in organ culture by full-thickness human skin explants exposed to the irritant sulfur mustard. J Invest Dermatol 1991;96:888–897.
18. Zhang Z, Riviere JE, Monteiro-Riviere NA. Topical sulfur mustard induces changes in prostaglandins and interleukin-1α in isolated perfused porcine skin. In Vitro Toxicol 1995;8:149–158.
19. Tanaka F, Dannenberg AM, Higuchi K, Nakamura M, Pula PJ, Hugli TE, Discipio RG, Kreutzer DL. Chemotactic factors released in culture by intact developing and healing skin lesions produced by the irritant sulphur mustard. Inflammation 1997;21:251–267.
20. Pu Y, Lin P, Vaughn FL, Bernstein IA. Appearance of interleukin 1α relates DNA interstrand cross-links and cytotoxicity in cultured human keratinocytes exposed to bis-(2-chloroethyl)sulfide. J Appl Toxicol 1995;15:477–482.
21. Kurt EM, Schafer RJ, Broomfield CA, Kahler DW, Arroyo CM. Immunologic cytokine expression in human keratinocytes after exposure to sulfur mustard. J Am Coll Toxicol 1997;15:S32–S35.
22. Lardot C, Dubois V, Lison D. Sulfur mustard upregulates the expression of interleukin-8 in cultured human keratinocytes. Toxicol Lett 1999;110:29–33.
23. Arroyo CM, Schafer RJ, Kurt EM, Broomfield CA, Carmichael AJ. Response of normal human keratinocytes to sulfur mustard (HD): cytokine release using a non-enzymatic detachment procedure. Hum Exp Toxicol 1999;18:1–11.
24. Imaizumi T, Nomura K, Hashimoto I, Sawada Y. Interleukin-1 levels in blister fluids of some skin diseases with blister formation. Clin Physiol Biochem 1990;8:179–183.
25. Barker JNWN, Mitra RS, Griffiths CEM, Dixit VM, Nickoloff BJ. Keratinocytes as initiators of inflammation. Lancet 1991;337:211–214.

26. Ameglio F, Bonifati C, Pietravalle M, Fazio M. Interleukin-6 and tumor necrosis factor levels decrease in the suction blister fluids of psoriatic patients during effective therapy. Dermatology 1994;189:359–363.
27. Gupta S, Sauder DN. The skin as an immune organ: the role of keratinocyte. U Toronto Med J 1995;72:118–123.
28. Ming WJ, Bersani L, Mantovani A. Tumor necrosis factor is chemotactic for monocytes and polymorphonuclear leukocytes. J Immunol 1987;138:1469–1474.
29. Yong KL, Linch DC. Granulocyte-macrophage-colony-stimulating factor differentially regulates neutrophil migration across IL-1-activated and nonactivated human endothelium. J Immunol 1993;150:2449–2456.
30. McAdams AJ. A study of mustard vesication. J Invest Dermatol 1956;26:317–326.
31. Chauhan RS, Murthy VR, Arora U, Malhotra PR. Structural changes induced by sulphur mustard in rabbit skin. J Appl Toxicol 1996;16:491–495.
32. Petrali JP, Oglesby-Megee SB. Toxicity of mustard gas lesions. Microsc Res Tech 1997;37:221–228.
33. Brown RFR, Rice P. Histopathological changes in Yucatan minipig skin following challenge with sulphur mustard: a sequential study of the first 24 hours following challenge. Int J Exp Pathol 1997;78:9–20.
34. Zlotogorski A, Glodenhersh M, Shafran A. A model for quantitative measurement of sulphur mustard skin lesions in the rabbit ear. Toxicology 1997;120:105–110.
35. Monteiro-Riviere NA, Inman AO, Babin MC, Casillas RP. Localization of nine epidermal-dermal junction epitopes in the mouse ear exposed to bis(2-chloroethyl)sulfide. J Appl Toxicol 1999;19:313–328.
36. Ohta Y, Nishiyama S, Nishioka K. In situ expression of interleukin-6 in psoriatic epidermis during treatment. J Dermatol 1994;21:301–307.
37. Nurnberg W, Haas N, Schadendorf D, Czarnetzki BM. Interleukin-6 expression in the skin of patients with lupus erythematosus. Exp Dermatol 1995;4:52–57.
38. Boehm, KD, Yun JK, Strohl KP, Elmets CA. Messenger RNAs for the multifunctional cytokines interleukin-1 alpha, interleukin-1 beta and tumor necrosis factor-alpha are present in adnexal tissues and in dermis of normal human skin. Exp Dermatol 1995;4:335–341.
39. Ahmed AA, Nordlind K, Schultzberg M, Liden S. Proinflammatory cytokines and their corresponding receptor proteins in eccrine sweat glands in normal and cutaneous leishmaniasis human skin: an immunohistochemical study. Exp Dermatol 1996;5:230–235.
40. Ahmed AA, Nordlind K, Schultzberg M, Brakenhoff J, Bristulf J, Novick D, Svenson SB, Azizi M, Liden S. Immunohistochemical studies of proinflammatory cytokines and their receptors in hair follicles of normal human skin. Acta Derm Venereol 1996;76:348–352.
41. Casillas RP, Kiser RC, Truxall JA, Blank JA, Singer AW, Ricketts KM, Mitcheltree LW, Stemler FW. Therapeutic approaches to dermatotoxicity by sulfur mustard: part I. Modulation of sulfur mustard-induced cutaneous injury in the mouse ear vesicant model (MEVM). J Appl Toxicol, in press.
42. Babin MC, Ricketts K, Skvorak JP, Gazaway M, Mitcheltree LW, Casillas RP. Systemic administration of candidate antivesicants to protect against topically applied sulfur mustard in the mouse ear vesicant model (MEVM). J Appl Toxicol, in press.
43. Vojvodic V, Milosavljevic Z, Boskovic B, Bojanic N. The protective effect of different drugs in rats poisoned by sulfur and nitrogen mustards. Fund Appl Toxicol 1985;5:160–168.
44. Vijayaraghavan R, Sugendran K, Pant SC, Husain K, Malhotra RC. Dermal intoxication of mice with bis(2-chloroethyl) sulphide and the protective effect of flavonoids. Toxicology 1991;69:35–42.
45. Vogt RF, Dannenberg AM, Schofield BH, Hynes NA, Papirmeister B. Pathogenesis of skin lesions caused by sulfur mustard. Fund Appl Toxicol 1984;4:71–83.
46. Ballantyne B. Intramuscular prednisolone pretreatment does not influence the dermal lesions induced by the topical sulfur mustard. Vet Hum Toxicol 1986;28:204–206.
47. Yourick JJ, Clark CR, Mitcheltree LW. Niacinamide pretreatment reduces microvesicle formation in hairless guinea pigs cutaneously exposed to sulfur mustard. Fund Appl Toxicol 1991;17:533–542.
48. Yourick JJ, Dawson JS, Benton CD, Craig ME, Mitcheltree LW. Pathogenesis of 2,2'-dichlorodiethyl sulfide in hairless guinea pigs. Toxicology 1993;84:185–197.
49. Yourick JJ, Dawson JS, Mitcheltree LW. Reduction of erythema in hairless guinea pigs after cutaneous sulfur mustard vapor exposure by pretreatment with niacinamide, promethazine and indomethacin. J Appl Toxicol 1995;15:133–138.
50. Mol MAE, De Vries R, Kluivers AW. Effects of nicotinamide on biochemical changes and microblistering induced by sulfur mustard in human skin organ cultures. Toxicol Appl Pharmacol 1991;107:439–449.
51. Zhang Z, Riviere JE, Monterio-Riviere NA. Evaluation of protective effects of sodium thiosulfate, cysteine, niacinamide and indomethacin on sulfur mustard-treated isolated perfused porcine skin. Chem Biol Interact 1995;96:249–262.